NANO LETTERS

Letter

pubs.acs.org/NanoLett

Subnanometer Ga_2O_3 Tunnelling Layer by Atomic Layer Deposition to Achieve 1.1 V Open-Circuit Potential in Dye-Sensitized Solar Cells

Aravind Kumar Chandiran,* Nicolas Tetreault, Robin Humphry-Baker, Florian Kessler, Etienne Baranoff,† Chenyi Yi, Mohammad Khaja Nazeeruddin,* and Michael Grätzel*

Laboratory of Photonics and Interfaces, Institute of Chemical Sciences and Engineering, Swiss Federal Institute of Technology (EPFL), Station 6, 1015 Lausanne, Switzerland.

Supporting Information

ABSTRACT: Herein, we present the first use of a gallium oxide tunnelling layer to significantly reduce electron recombination in dye-sensitized solar cells (DSC). The subnanometer coating is achieved using atomic layer deposition (ALD) and leading to a new DSC record open-circuit potential of 1.1 V with state-of-the-art organic D-π-A sensitizer and cobalt redox mediator. After ALD of only a few angstroms of Ga_2O_3, the electron back reaction is reduced by more than an order of magnitude, while charge collection efficiency and fill factor are increased by 30% and 15%, respectively. The photogenerated exciton separation processes of electron injection into the TiO_2 conduction band and the hole injection into the electrolyte are characterized in detail.

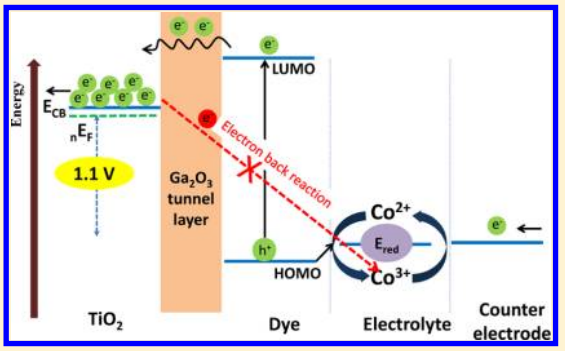

KEYWORDS: *Atomic layer deposition, dye-sensitized solar cell, gallium oxide, tunnelling layer, electron recombination*

Dye-sensitized solar cells (DSC) have attracted considerable attention from the energy market and researchers alike thanks to the flexibility it offers in terms of material selection, low cost, and chemical stability.[1−7] The electrochemical system is sandwiched between two transparent conductive oxide (TCO) glass substrates and comprises a printed dye-sensitized mesoporous titania (TiO_2) film infiltrated with a redox electrolyte and a platinum-coated counter electrode. Solar photons with an energy equal to or greater than the HOMO−LUMO gap of the dye are absorbed generating electron−hole (e^-_{photo}−h^+_{photo}) pairs. These excitons are separated at the titania−sensitizer−electrolyte interfaces where the electrons are injected into the TiO_2 conduction band and the holes into the electrolyte.[1,2] While the cell's short-circuit photocurrent density (J_{SC}) is mainly determined by the light harvesting ability of the dye over the visible light spectrum, the open-circuit potential (V_{OC}) of the device is determined by the difference between two energetic positions: the quasi-Fermi level ($_nE_F$) of electrons in the TiO_2 and the redox potential of the electrolyte medium. At open-circuit, the rate of e^-_{photo} injection into the TiO_2 is equal to the rate of recombination with the oxidized form of the redox couple, while the steady-state electron density (n_c) in the TiO_2 film determines the position of $_nE_F$. For a given redox potential, slower recombination kinetics shifts the $_nE_F$ toward the conduction band of TiO_2 leading to an increase in V_{OC}.[8,9]

Recently, research efforts have shifted from the development of panchromatic Ru(II) polypyridyl sensitizers regenerated using the standard iodide/triiodide (I^-/I_3^-) electrolyte to organic or phorphyrin dyes with finely tuned electron donor, π-bridge, and acceptor groups coupled with alternative single electron redox shuttles, like disulfide/thiolate, ferrocene, or cobalt complexes to achieve new record power conversion efficiencies (PCE) of 12.3% at 1 sun and 13.1% at 0.5 sun.[10−15] Cobalt complex-based redox mediators offer tunable redox potentials and require less dye regeneration overpotentials to significantly enhance the V_{OC}.[16] In spite of these advantages, $Co^{(II/III)}$ complexes suffer from faster recombination dynamics of photogenerated electrons with the oxidized species in the electrolyte than that of the two electron iodide/triiodide limiting potential gains in V_{OC} and overall PCE.[12,16−18]

Thin metal oxides films have been shown in the past to efficiently passivate surface states and block the back reaction. However, conventional solution-based passivation techniques often lead to the formation of inhomogeneous films thicker than ≈1 nm which significantly hampers electron injection into the TiO_2 conduction band.[19−22] The recent development of atomic layer deposition (ALD) for the growth of ultrathin conformal films on high aspect ratio nanostructures, down to atomic layer thickness, has compelled DSC researchers to revisit this strategy.[23−27] ALD is a self-limited growth process determined by the density of reactive sites on host's surface. To summarize, the organometallic precursor and oxidizing agent are pulsed subsequently into a vacuum chamber using an inert gas as carrier to effectively avoid gas-phase reaction in the reactor, preventing the formation of thick oxide layers.[28,29] However, previous reports on TiO_2 passivation by ALD of

Received: March 15, 2012
Revised: May 27, 2012
Published: June 11, 2012

   dx.doi.org/10.1021/nl301023r | *Nano Lett.* 2012, 12, 3941−3947

ZrO_2, HfO_2, and Al_2O_3 in I^-/I_3^- based DSC showed a significant decrease in J_{SC} without the significant V_{OC} improvement associated with an effective blocking of the recombination pathway leading to a decrease in the overall power conversion efficiency (PCE).[23−27] With that said, Snaith et al.[30] and Li et al.[27] have shown that MgO and ZrO_2 overlayers, respectively, could slightly improve all the photovoltaic parameters in low-efficiency solid-state DSC using an organic hole transport material. In addition, Tetreault et al.[31,32] have been able to improve all photovoltaic parameters using TiO_2-passivation of Al-doped ZnO and SnO_2 in a I^-/I_3^- based DSC, owing to a small reduction in recombination and a shift in the conduction band. However, to achieve true tunnelling behavior, there should be no available density of states between the dye excited state (S*) and conduction band (CB) of the electron accepting material. Theoretically, the tunneling process can only occur through a barrier material, that possesses a larger bandgap, due to the strong electric field between the S* and CB.[33] Considering the compromises and limitations described in the literature, we present herein a novel strategy using a highly insulating subnanometer gallium oxide (Ga_2O_3, −2.95 eV vs vacuum) ALD overlayer as tunnelling barrier to effectively balance injection and recombination in DSCs.[34,35] The insulating Ga_2O_3 was also selected due its ability to form conformal layer on the mesoporous TiO_2, unlike Al_2O_3 where the deposition progresses following an island growth mode.[36] In conjunction with a state-of-the-art organic D-π-A dye (Y123)[11] and a novel single electron Co(bipyridine-pyrazole) redox mediator,[37] we present a new record open-circuit potential of 1.1 V coupled to an increase in J_{SC} and fill factor (ff) in the device. Through a complete characterization of the electron-transfer processes, we show that this is primarily due to an order of magnitude reduction in the recombination kinetics and an increase in electron collection efficiency.

Experimental details for the photoanode preparation, ALD, photovoltaic and material characterization as well as the electrochemical impedance spectroscopy (EIS) and photo-induced absorption (PIA) conditions are presented in the experimental section of the Supporting Information.

Different numbers of ALD cycles of Ga_2O_3 were deposited into a 2.7 ± 0.1 μm thick mesoporous TiO_2 film in a highly conformal manner using sequential exposures to tris(dimethyl) amido gallium and H_2O.[38] A relatively thin TiO_2 film thickness was chosen to ensure uniform Ga_2O_3 deposition throughout the film and was limited by the diffusion length of the metal organic precursor in the mesopores. The reference (0 cycle) and the Ga_2O_3-passivated TiO_2 samples were characterized using X-ray photoelectron spectroscopy. Both the reference and passivated films show two binding energy peaks at 459.45 ± 0.15 and 465.05 ± 0.1 eV, corresponding to the Ti $2p_{3/2}$ and Ti $2p_{1/2}$ transitions (Figure 1 inset), respectively, indicating that the Ti^{4+} oxidation state is preserved after passivation.[39] In addition, a peak at 1118.65 ± 0.1 eV is observed for the surface treated films that is assigned to the Ga $2p_{3/2}$ transition confirming the presence of the Ga^{3+} valence state expected for Ga_2O_3 (Figure 1).[40] It can be noted that the Ga $2p_{3/2}$ binding energy peak intensity increases with the number of ALD cycles and, hence, the increase of Ga content on the surface. The growth rate of Ga_2O_3 by ALD was estimated to be ∼1 Å per cycle by spectroscopic ellipsometry on Si wafer covered using the same ALD conditions. However, the growth rate for the first few cycles will be dependent on the surface chemistry of the host material, and thus, we should expect some deviation of the growth rate of Ga_2O_3 on the Si native oxide and that on TiO_2.[41]

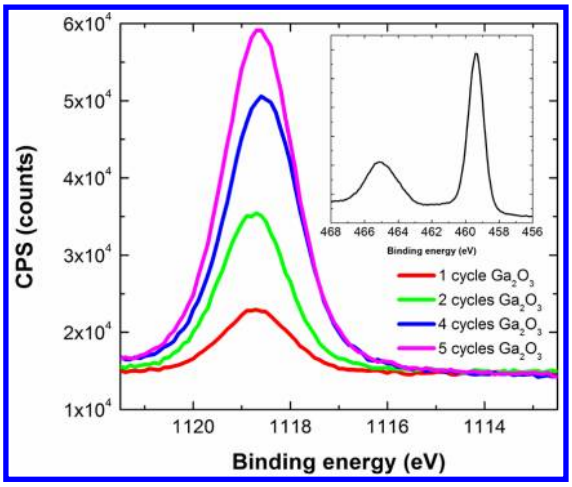

Figure 1. X-ray photoelectron spectra of the Ga $2p_{3/2}$ transition (1118.65 ± 0.1 eV) confirming the presence of the Ga^{3+} valence state expected for Ga_2O_3. The transition peak intensity is found to increase together with the number of Ga_2O_3 ALD cycles. (Inset) Ti $2p_{3/2}$ and Ti $2p_{1/2}$ transitions (459.45 ± 0.15, 465.05 ± 0.1 eV) for the Ti^{4+} oxidation state preserved after addition of the tunnelling overlayer.

To test the performance of the tunnelling overlayer in DSCs, mesoporous TiO_2 photoanodes printed on a fluorine-doped tin oxide (FTO) glass substrate were covered by ALD of Ga_2O_3, covering both the TiO_2 host and the exposed FTO surface. Then, the photoanodes were sensitized with Y123 (Figure 2A) and infiltrated with the Co(bipyridine-pyrazole)$^{2+/3+}PF^-_6$ redox mediator (Figure 2B). This dye and electrolyte combination was chosen specifically for the high molar extinction coefficient of the D-π-A Y123 sensitizer (48 000 M^{-1} cm^{-1}) and the standard redox potential of the Co(bipyridine-pyrazole)$^{2+/3+}$ (0.86 V vs NHE), enabling efficient light harvesting and high open-circuit potential, respectively.[11,37] Figure 3 shows the $J-V$ performance of these cells as measured in the dark and at full sun (AM 1.5G). The onset of the dark current for the reference cell (black dashed curve) is observed at about 400 mV and is increased by about 500 mV, to 900 mV, upon deposition of 4 Ga_2O_3 ALD cycles (blue dashed line) to significantly block dark current generation. Under full illumination, the $J-V$ characteristics of the reference cell were found to be V_{OC} = 692 mV, J_{SC} = 3.6 mA/cm^2, and ff = 56.0%, leading to a modest PCE of 1.4% (black solid line). A substantial increase in V_{OC} to 1000 mV is obtained after 1 Ga_2O_3 ALD cycle (red solid line) before reaching the record-breaking photovoltage of 1100 mV after 4 ALD cycles (blue solid line). In addition, we found that both the photocurrent and the ff increased to J_{SC} = 5.1 mA/cm^2 and ff = 70.8% to increase the cell efficiency to reach PCE = 4.0%. Further Ga_2O_3 deposition only slightly raised the V_{OC} to 1118 mV at a great expense for the J_{SC} that is significantly decreased to 2.8 mA/cm^2 after 6 ALD cycles (dark-yellow solid line). The full $J-V$ characteristics and efficiencies are presented in Table 1. Finally, in order to better deconvolute the effects of photovoltage loss at the FTO-electrolyte and TiO_2-electrolyte interfaces, a 5 nm thick TiO_2 blocking underlayer was deposited on the FTO-glass to avoid contact with the electrolyte. The complete photovoltaic properties of the cells were investigated after a different number of cycles of Ga_2O_3 deposition covering both the mesoporous film and the underlayer.[42] The $J-V$ curves are presented in Figure S1, Supporting Information, and

dx.doi.org/10.1021/nl301023r | Nano Lett. 2012, 12, 3941−3947

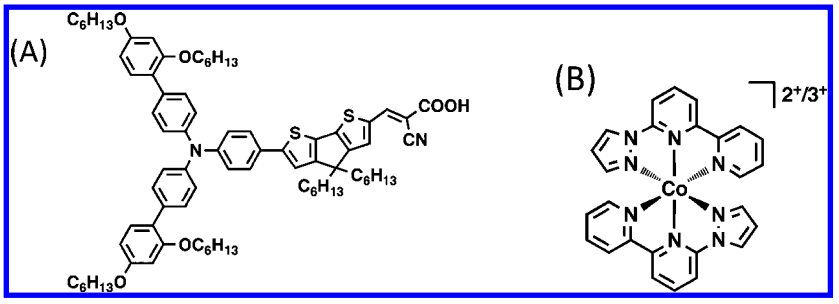

Figure 2. (A) Molecular structure of the organic D-π-A sensitizer coded as Y123. (B) Molecular structure of Co(bipyridine-pyrazole)$^{2+/3+}$ PF_6^- redox mediator used in the present DSCs.

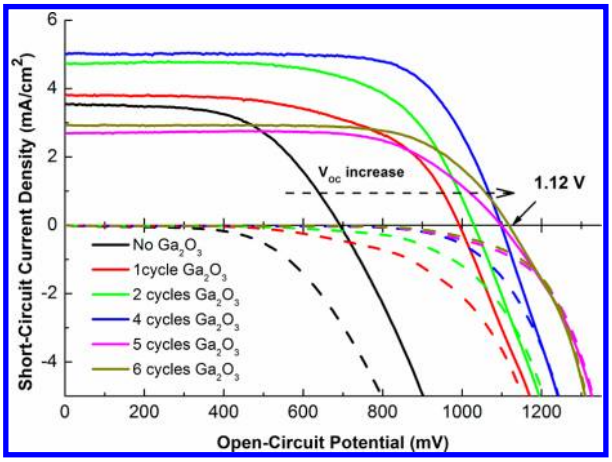

Figure 3. Photocurrent−voltage (J−V) characteristics for DSC photoanodes subjected to different number of Ga_2O_3 ALD cycles as well as for the bare reference (black). Solid and dashed lines correspond to measurements under simulated AM1.5G solar irradiance (100 mW cm^{-2}) and in the dark, respectively.

Table 1. Photovoltaic Characteristics (J_{SC}, V_{OC}, ff, and PCE) for Photoanodes with Different Numbers of Ga_2O_3 ALD Cycles[a]

no. of Ga_2O_3 ALD cycles	J_{SC} (mA/cm^2)	V_{OC} (mV)	ff (%)	PCE (%)
0	3.6	692	56.0	1.4
1	4.9	995	62.7	3.2
2	4.8	1030	63.8	3.2
4	5.1	1098	70.8	4.0
5	2.7	1099	67.2	2.0
6	2.9	1118	68.6	2.3

[a]Reference = 0 cycle. Experimental errors are within ±10 mV for V_{OC}, ± 0.2 mA/cm^2 for J_{SC}, and ±0.5% for ff.

the corresponding photovoltaic data are presented in Table S1, Supporting Information. Although the V_{OC} (1022 mV) of the cell with underlayer and without Ga_2O_3 was found to be higher than the reference cell. The blocking behavior of the TiO_2 was found to have a lesser effect than the tunnelling behavior obtained with Ga_2O_3. The increase in the V_{OC} to 1070−1100 mV is observed with the simultaneous enhancement of the J_{SC} and the ff up to 3−4 cycles of Ga_2O_3. This shows that the back reaction is predominant at the FTO−electrolyte interface with a significant fraction observed at the TiO_2−electrolyte interface. However, the presence of tunneling Ga_2O_3 layer is found to suppress the back reaction at both the interfaces. The increase in the J_{SC} in the latter case is supported by the incident photon-to-electron conversion efficiency (IPCE) shown in Figure S2, Supporting Information.

This dramatic increase of the open-circuit potential (Table 1) could be explained by a reduction of the trap-state density of the TiO_2 or reduction of the recombination rate between electrons in the TiO_2 and the oxidized form of the redox couple. However, no significant modification of the density of trap states upon Ga_2O_3 ALD could be measured using transient photocurrent measurements. But, the ability of the Ga_2O_3 overlayer to significantly decrease the recombination kinetics was revealed by transient photovoltage decay measurements.[8,43,44] Figure 4A shows the recombination rate measured at different open-circuit potential obtained by varying the light bias on the cells. At the operating voltage, one Ga_2O_3 ALD cycle (red dots) is found to decrease the recombination rate by

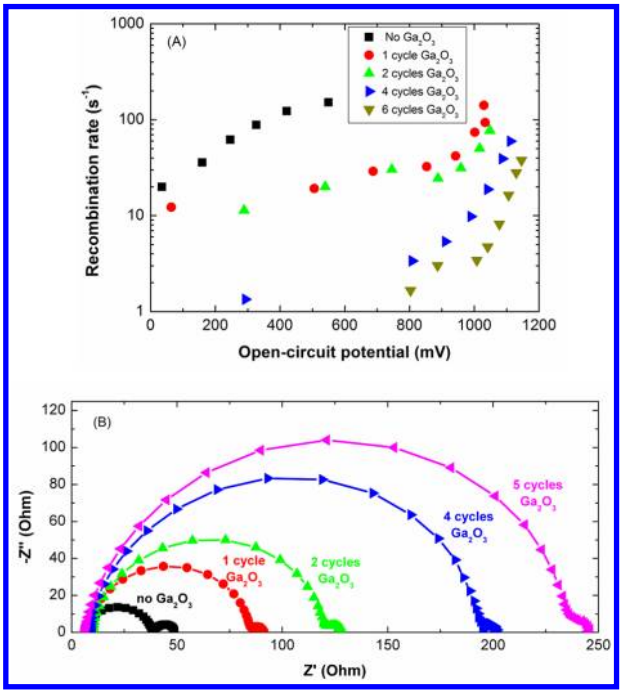

Figure 4. (A) Transient photovoltage decay measurements showing the recombination rate of photogenerated electrons as a function of open-circuit potentials for DSCs with different numbers of Ga_2O_3 ALD cycles as well as for the reference. (B) Nyquist plot showing the evolution of the high-frequency semicircle corresponding to the interfacial charge-transfer resistance (R_{CT}) for mesoporous TiO_2 photoanodes with no Ga_2O_3 tunnelling overlayer and after different numbers of Ga_2O_3 ALD cycles. The measurements were carried out at 0.55 V forward bias in the dark with a cell configuration analogous to the DSC but without a sensitizer.

dx.doi.org/10.1021/nl301023r | Nano Lett. 2012, 12, 3941−3947

about 1 order of magnitude compared to the reference cell (black squares). Further increase in the overlayer thickness decreases the rate of electron transfer to the Co^{3+} by another order of magnitude up to the sixth ALD cycle. Hence, the 2 orders of magnitude improvement in the lifetime (recombination rate^{-1}) of the photogenerated electrons at open circuit increases the steady-state electron density in the TiO_2, shifting the quasi-Fermi level toward vacuum and leading to a dramatic increase of the V_{OC} from 692 to 1120 mV.

This was confirmed by EIS to further analyze the recombination kinetics of the reference and Ga_2O_3-passivated photoanodes at the oxide−electrolyte interface.[45] Figure 4B compares the Nyquist plot of the two photoanodes measured at 0.550 V forward bias in the dark. All spectra exhibit a high-frequency semicircle that corresponds to the interfacial charge-transfer resistance (R_{CT}) and a low-frequency semicircle attributed to the diffusion resistance of Co^{3+} toward the counter electrode. The high-frequency semicircle was fitted to a Randles equivalent circuit shown in Figure S3, Supporting Information to extract R_{CT}.[46] The R_{CT} for the reference cell was calculated to be 32.3 Ω and found to steadily increase with each Ga_2O_3 ALD cycle to reach R_{CT} = 230.7 Ω. This trend of increasing R_{CT} correlates well with the transient photovoltage decay measurements where the recombination rate was found to decrease significantly with each additional ALD cycle and further confirms that the gain in potential is a result of considerable reduction in the recombination kinetics at the photoanode.

The recombination rate of electrons in the cells with the ALD TiO_2 underlayer is presented in Figure S4, Supporting Information, as the function of voltage. We can see that the increase in the number of cycles of Ga_2O_3 deposition decreases the recombination rate, which confirms the suppression of the back reaction from the TiO_2-electrolyte interface and the trend is consistent with recombination shown in Figure 4.

Figure S5A, Supporting Information shows the absorption spectra of the reference and Ga_2O_3-passivated photoanodes after sensitization with Y123. It can be seen that both films exhibit similar absorption profiles, and their intensities are the same within the experimental error. This result confirms that the dye uptake is unaffected by the Ga_2O_3 passivation of the TiO_2 surface but does not explain the 42% increase in J_{SC} observed (Table 1). To help understand this increase, the IPCE was measured for the reference and passivated DSCs over the range of wavelengths from 350 to 700 nm (Figure 5). The cell made with bare titania exhibits an absorbance rise from 380 nm with the maximum over a 400−600 nm range before falling back to 0 at 650 nm. The IPCE of the Ga_2O_3-treated film shows a similar profile but with an increased maximum close to 50%. The trend observed with IPCE matches that of the J_{SC}, and the integrated current from the spectra correlates closely with the photovoltaic data.

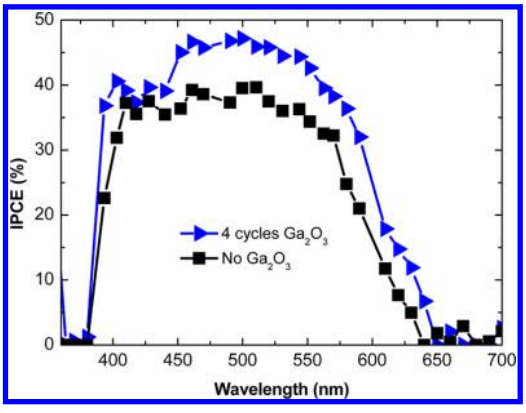

Figure 5. IPCE as a function of wavelength for DSC electrodes with and without the Ga_2O_3 tunneling overlayer (4 ALD cycles).

The IPCE is defined by four optical and electron-transfer factors which are the light harvesting efficiency (Φ_{LHE}), electron injection efficiency (Φ_{inj}), dye regeneration efficiency (Φ_{reg}) and charge collection efficiency (Φ_{coll}):[15]

$$IPCE = \Phi_{LHE}\Phi_{inj}\Phi_{reg}\Phi_{coll} \quad (1)$$

To rationalize the increase in IPCE for the Ga_2O_3-passivated TiO_2, these four parameters are analyzed separately. The light harvesting efficiency is calculated from the absorption spectra on the sensitized TiO_2 films (Figure S5B, Supporting Information). The Φ_{LHE} is found to be close to 100% for both the bare and the surface passivated TiO_2 from 350 to 500 nm and drops following the trend of the absorption spectrum. Since the Φ_{LHE} is found to be similar for both the photoanodes, this parameter cannot properly explain the observed increased in IPCE upon passivation. The absorbed photon-to-electron conversion efficiency (APCE) is cumulatively defined by the last three parameters in eq 1 giving the true quantum yield of photocurrent:

$$APCE = IPCE/\Phi_{LHE} = \Phi_{inj}\Phi_{reg}\Phi_{coll} \quad (2)$$

Figure S6, Supporting Information, shows the APCE calculated by dividing the IPCE by Φ_{LHE} follows the general profile of the IPCE. In order to analyze specifically the kinetics of the photoexcited electron injection into the conduction band of the semiconductor, the fluorescence decay of Y123 for the reference and Ga_2O_3-passivated TiO_2 is measured using time-resolved single photon counting (TRSPC) as proposed by S. E. Koops et al.[47,48] A qualitative comparison on the injection capability is made between the reference electrode and the electrode containing four cycles of Ga_2O_3. From Figure S7, Supporting Information, it can be seen that the fluorescence decay is faster for the reference cell (black curve) ,and when the Ga_2O_3 is introduced, the emission decay is slightly delayed (blue curve). The long-lived excited state of the dye indicates the reduction in the injection kinetics of photogenerated electrons in the semiconductor through the tunnelling overlayer. This clearly shows that the subnanometer thick Ga_2O_3 tunnelling overlayer does slow down the electron injection, but at the same time, it is reducing the recombination kinetics by about 2 orders of magnitude.[23,24]

The third parameter, the dye regeneration efficiency is investigated using intensity modulated photoinduced absorption spectroscopy (PIA).[44,49] Figure 6A compares the PIA spectra of the Y123 on TiO_2 and Ga_2O_3-passivated TiO_2 infiltrated with acetonitrile or the Co^{2+}/Co^{3+} redox electrolyte with an excitation wavelength of 470 nm and a frequency modulation of 36 Hz. For the reference photoanode in acetonitrile (black solid line), three distinct absorption peaks are observed at 672, 790, and 1540 nm in the differential PIA spectrum (red arrows) indicating the presence of the transient dye cations. When the Co^{2+}/Co^{3+} electrolyte medium is introduced (black dotted line), the absorption intensities of the corresponding cations drop owing to the rapid reduction of the oxidized dye by Co^{2+}. However, the peaks do not disappear

dx.doi.org/10.1021/nl301023r | Nano Lett. 2012, 12, 3941−3947

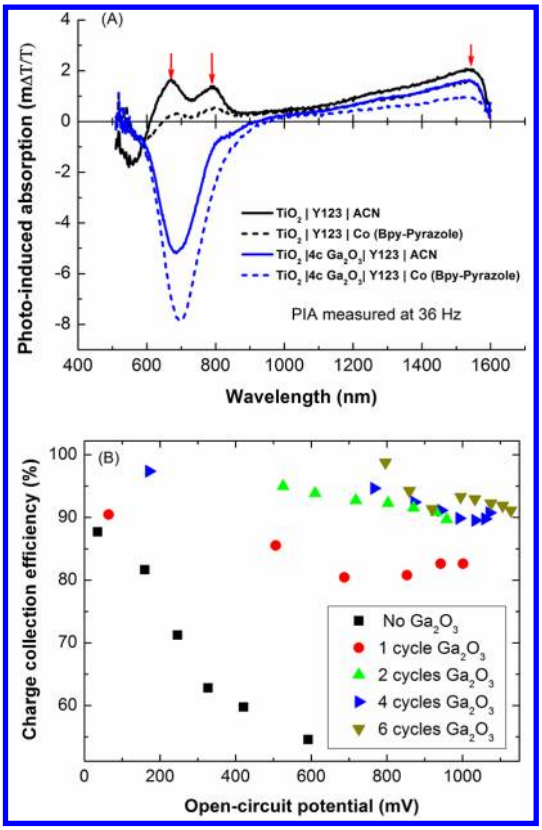

Figure 6. (A) PIA spectra of Y123 sensitized TiO_2 (black) and Ga_2O_3 passivated TiO_2 (blue) photoanodes infiltrated with acetonitrile (solid lines) and Co(bipyridine-pyrazole)$^{II/III}$ redox mediator (dashed lines). (B) Φ_{coll} as a function of open-circuit potentials (V_{OC}) for DSCs after different number of Ga_2O_3 ALD cycles as well as for the reference photoanode. Φ_{coll} is calculated from the ratio of transport rate and the sum of transport and recombination rates. All the cells described in this figure are made without a TiO_2 underlayer.

completely, which is indicative of incomplete regeneration. This might be due to the lower driving force for dye regeneration as well as poor electronic coupling between the dye and the bulky Co-complex.[16] When using the Ga_2O_3 tunnelling overlayer, a strong negative peak at 694 nm, a weak shoulder peak at 790 nm, and a positive absorption peak at 1540 nm are observed. The negative peak at 694 nm corresponds to the fluorescence decay of excited electrons from the LUMO to the HOMO now competing with the slowed down injection. The shoulder peak at 790 nm is representative of dye cation absorption as evidenced by the phase shift observed with respect to the modulated excitation shown in Figure S8, Supporting Information (solid blue line, red arrow). When the electrolyte is introduced, the shoulder peak disappears, and the peak intensity at 1540 nm is reduced indicating more efficient but still incomplete dye regeneration.

Finally, the charge collection efficiency[50] (Φ_{coll}) cumulatively takes into account the transport and recombination dynamics and is defined by the following equation:

$$\Phi_{coll} = 100 \times \text{transport rate}/(\text{transport rate} + \text{recombination rate}) \quad (3)$$

The plot of Φ_{coll} as a function of open-circuit potentials is shown in Figure 6B. For the reference cell at voltages close to 0, the Φ_{coll} is found to be about 90%. However, at operating voltages closer to 600 mV, the Φ_{coll} significant drops as low as 50%. With the deposition of just 1 Ga_2O_3 ALD cycle, the tunnelling layer is found to greatly enhance Φ_{coll}, which is maintained between 80 and 90% over all the voltages. With increasing thickness of the tunnelling overlayer, Φ_{coll} is further increased and remains above 90%. This improvement in the collection efficiency shows that the presence of the tunnelling layer prevents the loss of photogenerated electrons from the semiconductor to Co^{3+} at short-circuit.[43]

Thus, out of four parameters defining the IPCE, the Φ_{LHE} and Φ_{reg} have remained largely constant upon addition of the Ga_2O_3 tunnelling overlayer on the TiO_2 photoanodes. In contrast, an appreciable gain in charge collection efficiency dominates the loss in injection efficiency and serves to explain the significant increase in J_{SC} observed for DSCs that include the Ga_2O_3 tunnelling layer.[43]

In conclusion, the surface of the porous TiO_2 photoanode for DSC was passivated using a subnanometer thick Ga_2O_3 tunnelling overlayer by ALD. The numerous effects of the Ga_2O_3 were investigated in DSCs using a high molar extinction coefficient D-π-A organic sensitizer (Y123) and the state-of-the-art Co(bipyridine-pyrazole) redox electrolyte. The addition of the Ga_2O_3 tunnelling overlayer was found to increase the open-circuit potential of the device from 690 mV to a new record of 1.1 V after 4 ALD cycles. In addition, 42% and 15% increase in short-circuit current density and fill factor, respectively, were observed to improve the overall DSC efficiency at PCE = 4.0%. The remarkable increase in V_{OC} was shown using transient photovoltage decay and EIS to be caused by 2 orders of magnitude decrease of the recombination rate between electrons in the TiO_2 CB and the oxidized form of the redox couple. In spite of a small reduction in the electron injection efficiency after the addition of the tunnelling overlayer, the J_{SC} was increased due to a significant improvement in charge collection efficiency, which results from a decline in charge recombination at short-circuit. Further work on the ALD precursor chemistry to enhance the diffusion length in the mesopores will be necessary to implement this technological advance into thicker TiO_2 photoanodes in order to harvest the whole visible solar spectrum in high-efficiency DSCs. The decrease in the molecular size of the ALD metal precursors and the increase in the pore diameter of the mesoporous titania film by means of polymer additives can be considered as the possible options to augment the diffusion of precusors in the thicker photoanodes. The existing deposition technology can be directly implemented in the 1D nanowire-based solar cells as the precursors do not have to diffuse through the random pore orientation to cover the whole photoanode, like in the mesoporous structures. The development of this tunnelling overlayer opens a new parameter space of research on new single-electron redox mediators or hole transport materials suffering from fast recombination kinetics. This should allow this technology to break new grounds and reach higher efficiencies in both liquid and solid-state DSCs. However, the authors do not expect the system to enhance the open-circuit potential significantly with an iodide/triiodide electrolyte due to its slow two electron recombination process for the conversion of I_3^- to I^-.[8]

■ ASSOCIATED CONTENT

Supporting Information

The photovoltaic data table and curves for the solar cells with 5 nm TiO_2 underlayer, the corresponding IPCE plot, equivalent

dx.doi.org/10.1021/nl301023r | Nano Lett. 2012, 12, 3941−3947

circuit used to fit Nyquist plots representing the charge-transfer resistance, absorption and light harvesting efficiency spectra of dye-sensitized photoanodes, APCE spectrum, fluorescence decay, and photoinduced transient absorption spectra plots. This material is available free of charge via the Internet at http://pubs.acs.org.

AUTHOR INFORMATION

Corresponding Author

*aravindkumar.chandiran@epfl.ch; mdkhaja.nazeeruddin@epfl.ch; michael.graetzel@epfl.ch

Present Address

†School of Chemistry, University of Birmingham, Edgbaston, Birmingham, B15 2TT, United Kingdom.

Notes

The authors declare no competing financial interest.

ACKNOWLEDGMENTS

The authors acknowledge the financial contribution from EU FP7 project "ORION" grant agreement no. NMP-229036. This publication is partially based on work supported by the Center for Advanced Molecular Photovoltaics (award no. KUS-C1-015- 21), made by King Abdullah University of Science and Technology (KAUST). A.K.C. is grateful for financial support from the Balzan foundation as part of the 2009 Balzan Prize award to M.G. A.K.C. also thanks Dr. Hoi Nok Tsao and Dr. Aswani Yella for their valuable suggestions on electrolyte composition.

REFERENCES

(1) O'Regan, B.; Grätzel, M. *Nature* **1991**, *353*, 737.
(2) Grätzel, M. *Acc. Chem. Res.* **2009**, *42*, 1788.
(3) Law, M.; Greene, L. E.; Johnson, J. C.; Saykally, R.; Yang, P. *Nat. Mater.* **2005**, *4*, 455.
(4) Späth, M.; Sommeling, P. M.; van Roosmalen, J. A. M.; Smit, H. J. P.; van der Burg, N. P. G.; Mahieu, D. R.; Bakker, N. J.; Kroon, J. M. *Prog. Photovolt: Res. Appl.* **2003**, *11*, 207.
(5) Han, L.; Fukui, A.; Chiba, Y.; Islam, A.; Komiya, R.; Fuke, N.; Koide, N.; Yamanaka, R.; Shimizu, M. *Appl. Phys. Lett.* **2009**, *94*, 013305.
(6) Meyer, T. Turning the dye solar cell into an industrial product. Proceedings of the 3rd International Conference on the Industrialisation of DSC, DSC-IC 09, Nara, Japan, April 22–24, 2009; .
(7) Snaith, H. J.; Schmidt-Mende, L. *Adv. Mater.* **2007**, *19*, 3187.
(8) Peter, L. M. *Phys. Chem. Chem. Phys.* **2007**, *9*, 2630.
(9) Listorti, A.; O'Regan, B.; Durrant, J. R. *Chem. Mater.* **2011**, *23*, 3381.
(10) Nusbaumer, H.; Zakeeruddin, S. M.; Moser, J. E.; Grätzel, M. *Chem.—Eur. J.* **2003**, *9*, 3756.
(11) Tsao, H. N.; Yi, C.; Moehl, T.; Yum, J. H.; Zakeeruddin, S. M.; Nazeeruddin, Md.K.; Grätzel, M. *ChemSusChem* **2011**, *4*, 591.
(12) Feldt, S. M.; Gibson, E. A.; Gabrielsson, E.; Sun, L.; Boschloo, G.; Hagfeldt, A. *J. Am. Chem. Soc.* **2010**, *132*, 16714.
(13) Daeneke, T.; Kwon, T. H.; Holmes, A. B.; Duffy, N. W.; Bach, U.; Spiccia, L. *Nat. Chem.* **2011**, *3*, 211.
(14) Wang, M.; Chamberland, N.; Breau, L.; Moser, J. E.; Humphry-Baker, R.; Zakeeruddin, S. M.; Grätzel, M. *Nat. Chem.* **2010**, *2*, 385.
(15) Yella., A.; Lee, H. W.; Tsao, H. N.; Yi, Y.; Chandiran, A. K.; Nazeeruddin, Md.K.; Diau, E. W. G.; Yeh, C. Y.; Zakeeruddin, S. M.; Grätzel, M. *Science* **2011**, *334*, 629.
(16) Feldt, S. M.; Wang, G.; Boschloo, G.; Hagfeldt, A. *J. Phys. Chem. C.* **2011**, *115*, 21500.
(17) Nakade, S.; Kanzaki, T.; Kubo, W.; Kitamura, T.; Wada, Y.; Yanagida, S. *J. Phys. Chem. B.* **2005**, *109*, 3480.
(18) Nakade, S.; Makimoto, Y.; Kubo, W.; Kitamura, T.; Wada, Y.; Yanagida, S. *J. Phys. Chem. B.* **2005**, *109*, 3488.
(19) Kay, A.; Grätzel, M. *Chem. Mater.* **2002**, *14*, 2930.
(20) Palomares, E.; Clifford, J. N.; Haque, S. A.; Lutz, T.; Durrant, J. R. *J. Am. Chem. Soc.* **2003**, *125*, 475.
(21) Menzies, D.; Dai, Q.; Cheng, Y. B.; Simon, G. P.; Spiccia, L. *Mater. Lett.* **2005**, *59*, 1893.
(22) O'Regan, B. C.; Scully, S.; Mayer, A. C.; Palomares, E.; Durrant, J. *J. Phys. Chem. B* **2005**, *109*, 4616.
(23) Antila, L. J.; Heikkilä, M. J.; Aumanen, V.; Kemell, M.; Myllyperkiö, P.; Leskelä, M.; Korppi-Tommola, E. I. *J. Phys. Chem. Lett.* **2010**, *1*, 536.
(24) Antila, L. J.; Heikkilä, M. J.; Mäkinen, V.; Humalamäki, N.; Laitinen, M.; Linko, V.; Jalkanen, P.; Toppari, J.; Aumanen, V.; Kemell, M.; Myllyperkiö, P.; Karoliina, H.; Häkkinen, H.; Leskelä, M.; Korppi-Tommola, J. E. I. *J. Phys. Chem. C* **2011**, *115*, 16720.
(25) Hamann, T. W.; Farha, O. K.; Hupp, J. T. *J. Phys. Chem. C* **2008**, *112*, 19756.
(26) Law, M.; Greene, L. E.; Radenovic, A.; Kuykendall, T.; Liphardt, J.; Yang, P. *J. Phys. Chem. B* **2006**, *110*, 22652.
(27) Li, T. C.; Góes, M. S.; Fabregat-Santiago, F.; Bisquert, J.; Bueno, P. R.; Prasittichai, C.; Hupp, J. T.; Marks, T. J. *J. Phys. Chem. C* **2009**, *113*, 18385.
(28) George, S. M. *Chem. Rev.* **2010**, *110*, 111.
(29) Leskelä, M.; Ritala, M. *Thin solid films* **2002**, *409*, 138.
(30) Snaith, H. J.; Ducati, C. *Nano Lett.* **2010**, *10*, 1259.
(31) Tétreault, N.; Arsenault, É.; Heiniger, L.-P.; Soheilnia, N.; Brillet, J.; Moehl, T.; Zakeeruddin, S.; Ozin, G. A.; Grätzel, M. *Nano Lett.* **2011**, *11*, 4579.
(32) Tetreault, N.; Heiniger, L.-P.; Stefik, M.; Labouchère, P. P.; Arsenault, É.; Nazeeruddin, Md.K.; Ozin, G. A.; Grätzel, M. *ECS Trans.* **2011**, *41*, 303.
(33) Sze S. M. *Semiconductor Devices Physics and Technology*, 2nd ed.; Wiley-India: New Delhi, India, 2009.
(34) Shannon, R. D. *Acta Crystallogr.* **1976**, *A32*, 751.
(35) Hisatomi, T.; Formal, F. L.; Cornuz, M.; Brillet, J.; Tétreault, N.; Sivula, K.; Grätzel, M. *Energy Environ. Sci.* **2011**, *4*, 2512.
(36) Tien, T.-C.; Pan, F.-M.; Wang, L.-P.; Tsai, F.-Y.; Lin, C. *J. Phys. Chem. C* **2010**, *114*, 10048.
(37) Yum, J. H.; Baranoff, E.; Kessler, F.; Moehl, T.; Ahmad, S.; Bessho, T.; Marchioro, A.; Ghadiri, E.; Moser, J. E.; Yi, C.; Nazeeruddin, Md. K.; Grätzel, M. *Nat. Commun.* **2012**, *3*, 631.
(38) Dezelah, C. L.; Niinisto, J.; Arstila, K.; Niinisto, L.; Winter, C. H. *Chem. Mater.* **2006**, *18*, 471.
(39) Saied, S. O.; Sullivan, J. L.; Choudhury, T.; Pearce, C. G. *Vacuum* **1988**, *38*, 917.
(40) Schön, G. *J. Electron Spectrosc. Relat. Phenom.* **1973**, *2*, 75.
(41) Wang, J.; Baroughi, M. F.; Bills, B.; Galipeau, D.; Samadzadeh, R.; Sivoththaman, S. Proceedings of the 34th IEEE Photovoltaic Specialists Conference (PVSC), Philadelphia, PA,June 7–12, 2009; IEEE: Washington, D.C., 2009; p 001988
(42) Cameron, P. J.; Peter, L. M.; Hore, S. *J. Phys. Chem. B* **2005**, *109*, 930.
(43) O'Regan, B. C.; Durrant, J. R. *Acc. Chem. Res.* **2009**, *42*, 1799.
(44) Hagfeldt, A.; Boschloo, G.; Sun, L.; Kloo, L.; Pettersson, H. *Chem. Rev.* **2010**, *110*, 6595.
(45) Bisquert, J. *J. Phys. Chem. B* **2001**, *106*, 325.
(46) Fabregat-Santiago, F.; Bisquert, J.; Palomares, E.; Otero, L.; Kuang, D.; Zakeeruddin, S. M.; Grätzel, M. *J. Phys. Chem. C* **2007**, *111*, 6550.
(47) Koops, S. E.; O'Regan, B.; Barnes, P. R. F.; Durrant, J. R. *J. Am. Chem. Soc.* **2009**, *131*, 4808.
(48) Koops, S. E.; Durrant, J. R. *Inorg. Chim. Acta* **2008**, *361*, 663.
(49) Boschloo, G.; Hagfeldt, A. *Inorg. Chim. Acta* **2008**, *361*, 729.
(50) Chandiran, A. K.; Sauvage, F.; Casa-Cabanas, M.; Comte, P.; Zakeeruddin, S. M.; Graetzel, M. *J. Phys. Chem. C* **2010**, *114*, 15849.

NOTE ADDED AFTER ASAP PUBLICATION

This Letter was published ASAP on July 6, 2012. The Supporting Information has been modified. The correct version was published on July 24, 2012.

dx.doi.org/10.1021/nl301023r | *Nano Lett.* 2012, 12, 3941−3947